

Progress and Problems in QCD — Report from the Hadronic Final States Working Group at DIS99

Matteo Cacciari^a, Frank Chlebana^b, Laurel Sinclair^c and Marc Weber^d

^aCERN, Theory Division, CH-1211 Geneva 23, Switzerland.

^bFermi National Accelerator Laboratory, P.O. Box 500, Batavia, IL 60150, U.S.A.

^cDepartment of Physics and Astronomy, Glasgow University, Glasgow G12 8QQ, UK.

^d Institut für Hochenergiephysik, Universität Heidelberg, Schröderstraße 90, D-69120 Heidelberg, Germany.

We present a summary of the Hadronic Final States parallel sessions of the DIS99 workshop. Topics were presented over two days and included both theoretical and experimental talks. Recent progress in the understanding of QCD in deep inelastic scattering, e^+e^- collisions, and in γ and p collisions was discussed.

1. THEORY SUMMARY

During the parallel sessions of the Hadronic Final States Working Group about forty talks were presented. Out of these, about ten might be classified as theoretical ones. The issues they discussed ranged from instantons to heavy flavour production to higher order QCD calculations. It is therefore understandable how difficult it might be to try to provide an organic summary of such a widespread collection of interesting topics.

We shall therefore try to highlight here what we consider to be the main points of the various contributions, leaving the task of properly introducing and explaining the subject to the individual summaries. Such summaries will not be cited explicitly in this section, since they can easily be found in these proceedings under the name of the person who gave the presentation.

A common feature can be identified in almost all the talks given. They clearly focus on the need to go beyond standard fixed next-to-leading order (NLO) QCD perturbation theory as the quality of the experimental data demands more accurate theoretical calculations.

G. Salam and H. Jung both described phenomenological studies related to the CCFM equa-

tion. This is an evolution equation that goes beyond the so-called “multi-Regge” limit of the BFKL equation, and also tries to implement effects due to colour coherence (via angular ordering) and soft particles. As CCFM is harder to solve than BFKL, the question is how similar the predictions of the two approaches are. Salam argued that, with the inclusion of soft effects, BFKL and CCFM can be shown to lead to identical predictions at the leading log level. Differences at sub-leading level, as well as ambiguities in the implementation of the equations at this level, do however remain. Jung described a practical implementation of the CCFM equation in the program SMALLX and showed that a good phenomenological description of both F_2 and forward jets data can be achieved.

Small- x logarithms are not the only ones appearing in a QCD perturbative expansion. N. Kidonakis described how to take care of the large logs resulting from soft gluon emissions when final states are produced near threshold. Resummed expressions for these terms have been written some time ago, but until recently it was still unclear how to treat these expressions so that the final result would indeed only contain the resum-

mation of the perturbative series and not further spurious effects. In the approach that Kidonakis described, the resummed expression is truncated at next-to-next-to-leading order, i.e. one order beyond what is available as a full fixed order calculation. Due to the fairly good convergence properties of the series, such a treatment suffices to bring an improvement over the standard NLO calculation, and at the same time ensures consistency with the perturbative expansion.

One further resummation issue was addressed by S. Kretzer who described how charm effects in parton distribution functions, appearing at fixed order as $\log(Q/m)$, can be resummed using the ACOT scheme. He studied both neutral and charged current deep inelastic scattering (DIS). The difference between fixed order and resummed predictions does not seem to be within the reach of present experimental accuracy. It is however likely that such resummed approaches will be more and more important in the future, as experimental precision improves and larger scales are probed.

S. Frixione reviewed the status of theoretical calculations of heavy quark production. At small and moderate transverse momenta, NLO QCD calculations are available and reliable. In the large transverse momentum region, on the other hand, large logs of the form $\log(p_T/m)$ develop. Resummation techniques for such terms have been developed in recent years. By making use of the Altarelli-Parisi evolution of a perturbatively calculable heavy quark fragmentation function these logs are resummed to all orders. Inclusion of a non-perturbative parametrization for heavy quark hadronization effects, such as the Peterson fragmentation function, also provides a description of D^* photoproduction data. Frixione did however warn that this resummed calculation should not be used at too small transverse momentum values; a proper combination with the full fixed-order NLO massive calculation is necessary to make it reliable in this region.

A more exotic feature of QCD, namely instantons, which also go beyond perturbation theory, was discussed by F. Schrempp. Such objects, originating from the rich structure of the QCD vacuum, can in principle play an important role in

various long distance aspects of QCD. There are also short-distance implications. It was argued in this talk that in DIS at HERA there exists a potential for observing instanton-induced processes otherwise forbidden by usual QCD perturbation theory.

Back on more standard ground, D. Soper and M. Grazzini described efforts to produce calculations in fixed order perturbation theory. Soper described a numerical approach to one-loop computations: rather than evaluating each diagram analytically, all diagrams are properly added and the integrals involved are performed numerically, in such a way that the individual singularities cancel before integrating. The final result is therefore finite. This method has so far been successfully applied to the evaluation of the thrust distribution in e^+e^- collisions, but can in principle be extended to other processes. Grazzini reported on progress in perturbative calculations beyond the one-loop approximation. In particular, he described studies of the collinear limits of three partons, where generalizations of the Altarelli-Parisi splitting vertices appear. Such limits are one of the building blocks for next-to-next-to-leading calculations, the next frontier of perturbative QCD.

2. HEAVY QUARK PRODUCTION

Experimental results, both on charm and on bottom production, were presented by the ZEUS and H1 collaborations. Many D^* production data were updated from previous measurements. Heavy quarks can provide particularly interesting tests of perturbative QCD since, due to their large mass acting as a cutoff for infrared singularities, their total production rate can be predicted on rigorous theoretical grounds with no free parameters other than their mass, the parton distribution functions and the strong coupling.

The H1 collaboration showed that a generally good, albeit not perfect, agreement with NLO QCD predictions can be observed [1]. It is also worth noticing that the gluon distribution function in the proton has been extracted from charm data in both photoproduction and DIS. The two results show good agreement with each

other and with the indirect determination from F_2 , as shown in Fig. 1.

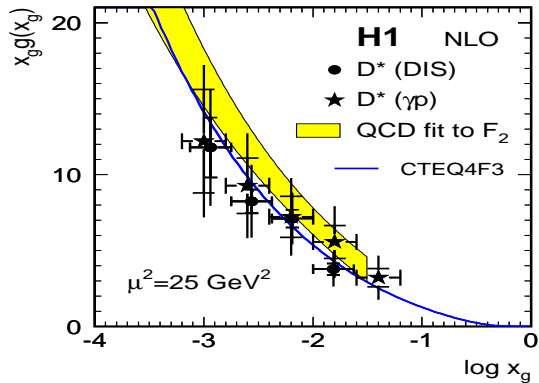


Figure 1. Gluon densities obtained from D^* analyses in photoproduction and DIS.

ZEUS D^* data were shown in a new low photon-proton energy region, $80 \text{ GeV} < W_{\gamma p} < 120 \text{ GeV}$ [2]. As shown in Fig. 2, the experimental data tend to be generally higher than the NLO QCD predictions, especially in the forward (proton) direction. Comparisons with the so-called massless approach show better agreement, but this kind of approach is probably not fully reliable at these low transverse momentum values [3].

Bottom production data, given in terms of observed leptons coming from semileptonic decays, were also presented by both ZEUS and H1 collaborations. ZEUS observed electrons, finding a cross section larger by a factor of ~ 4 than the one predicted by the HERWIG leading order (LO) plus parton shower Monte Carlo program [4]. H1 performed two analyses, both using muons to tag the heavy quark [5]. In these cases, the experimental results are about a factor of 5 and 3 larger than the prediction of a different LO Monte Carlo program, AROMA.

Such large factors between theory and experiment might seem important. However, one should keep in mind both the large errors still present in the experimental determinations and the fact that the theoretical prediction is given

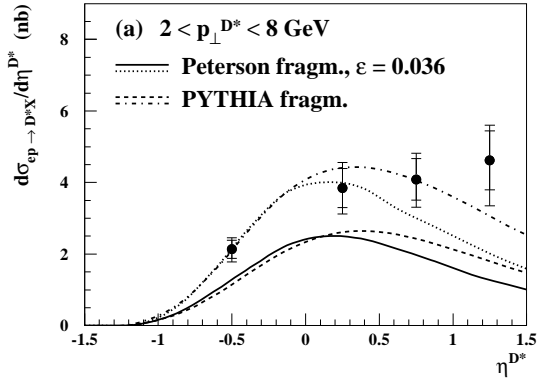


Figure 2. ZEUS differential cross sections $d\sigma/d\eta^{D^*}$ compared with NLO predictions for the massive approach. Full description of curves may be found in [2].

here by a leading order Monte Carlo program. It is well known that NLO calculations for heavy quarks greatly increase leading order predictions, usually by at least a factor of 2. However, a comparison with a NLO calculation is unfortunately not yet possible, since experimental results are only quoted for a “visible” cross section for which no full simulation at NLO is so far available. Combining this fact with the experimental uncertainty, it becomes apparent that it is still premature to talk of a discrepancy in the bottom production cross section at HERA. We are of course looking forward to more detailed comparisons between theory and experiment, bottom production being better behaved in QCD perturbation theory than charm, and therefore providing a better test of QCD predictions.

Heavy quark production was also discussed for the hidden flavour case, i.e. heavy quarkonia production. Elastic and inelastic J/ψ electroproduction has been analysed by the H1 collaboration [6]. Results from an inclusive sample (elastic plus inelastic) were compared to predictions from the so-called soft colour interaction model as implemented in the Monte Carlo program AROMA. Most of the shapes of the differential distributions can generally be reproduced, while the magnitude of the theoretical predictions is usually too low. Results from an inelastic sample were

instead compared to predictions obtained with the non-relativistic QCD (NRQCD) approach to quarkonium production. Such predictions can be seen to be at some variance with the data, both in magnitude and, especially for the rapidity distribution, in shape. It is however known that, especially at such a low scale as the one set by the charm mass, NRQCD predictions can suffer from large uncertainties.

3. JETS IN DIS

The use of jet algorithms and the study of jet-related observables continue to be both a popular and powerful approach in order to characterize the hadronic final state's properties. The analysis of multi-jet events in DIS has been used to extract the value of the strong coupling constant α_s [7, 8, 9, 10]. These and many other important analyses have clearly shown the large potential of QCD studies with jets at HERA but have also revealed important limitations. The latter are caused by the difficulties of current QCD Monte Carlo models to describe the data precisely, by the large renormalization scale uncertainties of QCD predictions in NLO in the phase space covered, or by the uncertainties of the proton's parton density.

In this session various presentations of jet analyses were given, which addressed these issues. Most analyses profited from the large data sample collected in particular during the very successful '97 data taking period of HERA. Thus, generally the measurements were considerably extended, either into the region of high photon virtuality, Q^2 , or to harder jet structures corresponding to large transverse jet energies, E_T^{Breit} , in the Breit frame. Three representative jet analyses are discussed in more detail below.

In [11] a systematic comparison of various measured jet distributions with model predictions was performed in dijet events at $Q^2 > 150 \text{ GeV}^2$. In Fig. 3 the x_p distribution determined with the modified Durham algorithm (run in the laboratory frame) is shown for three different ranges of Q^2 . The precision of the data is high and significant deviations of the QCD Monte Carlo models ARIADNE and LEPTO are observed. In contrast

to the MC models, the perturbative QCD predictions in NLO, which are also shown in Fig. 3, describe the measured jet distributions very well. The same conclusions are reached using the factorizable k_T algorithm (run in the Breit frame).

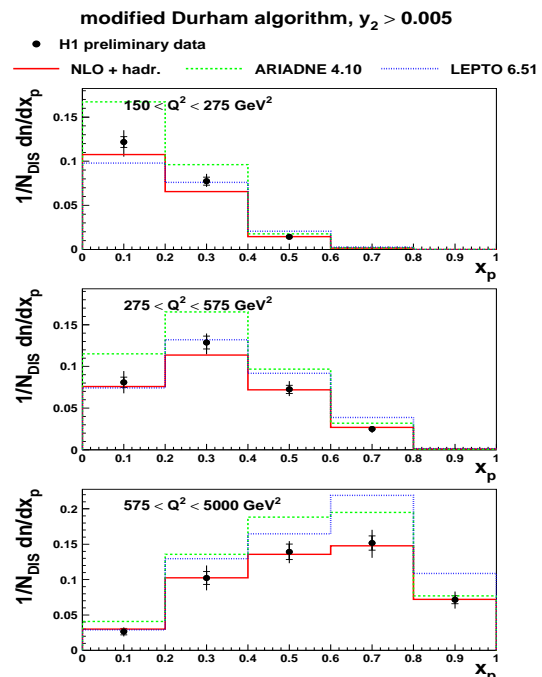


Figure 3. Distribution of $x_p = x_{Bj}/\xi$ in three ranges of Q^2 measured with the modified Durham algorithm.

It is important to note that both Monte Carlo models have recently been investigated in the context of the HERA Monte Carlo Workshop [12] and were considerably improved. In version 4.10 of ARIADNE, the Q^2 dependence of dijet events has been modified. In version 6.51 of LEPTO, a new model of soft-colour interactions has been implemented. Given the relative disagreement with the data, further development of the models is desirable.

An excellent description of the data by QCD in NLO is also observed in the preliminary inclusive jet cross sections, $d^2\sigma_{jet}/dE_T dQ^2$, in the kinematic region of $Q^2 > 150 \text{ GeV}^2$ and for

transverse jet energy $E_T^{Breit} > 7$ GeV [13]. In this phase space region both perturbative and non-perturbative uncertainties are expected to be small.

The corresponding dijet cross section measurements were fitted simultaneously with F_2 determinations to yield the gluon density of the proton [14]. This procedure extends the accessible range of the gluon momentum fraction, ξ , to larger values with respect to the less direct determinations of the gluon density from the scaling violation of F_2 . The value of the strong coupling constant was assumed to be known in this analysis, but a combined fit of both the gluon density and α_s should be possible in the future.

A preliminary measurement of the dijet event rate and the dijet cross section as a function of Q^2 and a determination of α_s were presented in [15]. Jets of high transverse momentum E_T^{Breit} have been selected at $Q^2 > 470$ GeV². In the region of large Q^2 , corresponding to large parton momentum fractions, the proportion of gluon-initiated scattering processes is minimal. Thus this analysis is less sensitive to the uncertainties in the gluon density and may depend to a lesser extent on the details of parton density extractions from the world data than earlier α_s determinations. Also, the renormalization scale uncertainties are (relatively) small, both owing to the large value of Q^2 and the high jet transverse energies required. Again, this nicely illustrates the quest for smaller (theoretical) uncertainties by selecting more restrictive but safer phase space regions.

4. EVENT SHAPES AND POWER CORRECTIONS

The comparison of exclusive hadronic final state observables with the corresponding perturbative QCD predictions requires an estimation of hadronization effects. Phenomenological models, such as the string or the cluster model implemented in Monte Carlo generators, are primarily used for these estimates. Depending on the observable under study, hadronization corrections may be large, however, and it is difficult to estimate their uncertainty rigorously.

An alternative approach consists in applying

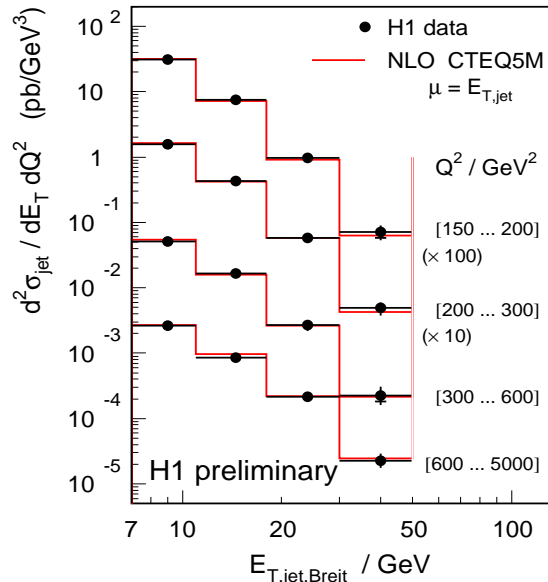


Figure 4. Inclusive jet cross section as a function of the transverse jet energy E_T in the Breit frame in different regions of Q^2 .

analytical power corrections of the form $\sim 1/Q^p$ when comparing perturbative QCD predictions with measured hadronic distributions. The leading power p and the exact form of the power corrections to the mean values of event shape distributions have been calculated for a large number of observables in both e^+e^- annihilation and deep inelastic scattering. The size of the correction depends on the value of an effective universal coupling constant $\bar{\alpha}_0$, on the strong coupling constant α_s and, of course, on Q^2 .

The results of a 2-parameter fit of α_s and $\bar{\alpha}_0$ to the mean values of various event shape distributions recently measured at HERA [16] are shown in Fig. 5. These results consider the recent theoretical developments of the calculation of two-loop corrections, leading to the so-called Milan factor [17], and of an updated calculation of the coefficient for the jet broadening variable [18]. Also, the experimental precision has been considerably improved with respect to an earlier analysis [19]. The value of $\bar{\alpha}_0$ is found to be ~ 0.5 and it is independent of the variable studied to within

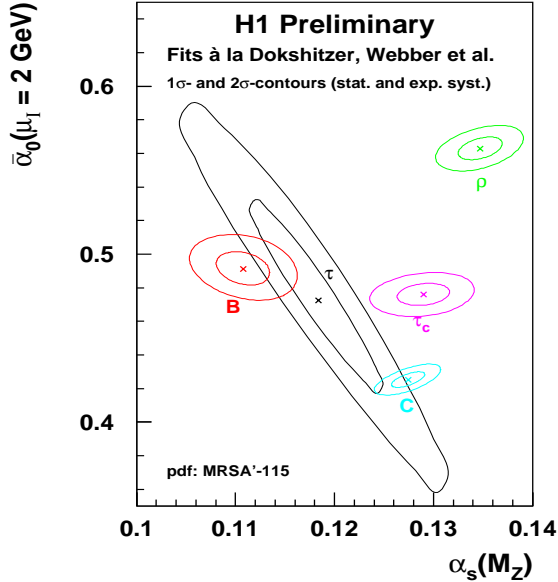


Figure 5. Determinations of $\alpha_s(M_Z)$ and $\bar{\alpha}_0$ for various event shape variables measured in DIS.

20%. The variation of the resulting α_s values is very large, however, which strongly suggests that further theoretical studies are needed.

In e^+e^- annihilation similar fits to the mean values (as a function of the centre-of-mass energy \sqrt{s}) of thrust, wide jet broadening and heavy jet mass yielded much better agreement in α_s and similar agreement in α_0 [20]. Predictions of power corrections to distributions, in contrast to mean values, of event shape observables have also been tested [20]. Fig. 6 shows the wide jet broadening distribution measured at different centre-of-mass energies. Perturbative QCD predictions with either hadronization corrections from Monte Carlo models (full line) or power corrections (dashed line) are fitted to the data and yield fits of similar quality to those without the power corrections but systematically lower values of α_s . The differences are largest at low centre-of-mass energy where also the applied corrections are sizeable.

In conclusion, the concept of power corrections has led to a remarkable theoretical activity, often in close collaboration with experimentalists, and

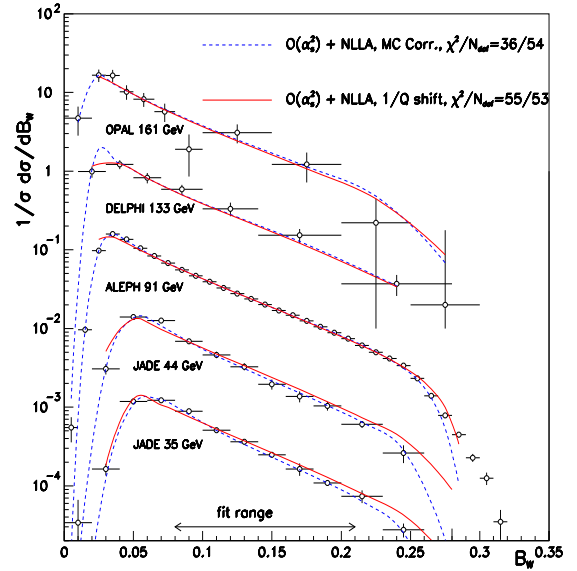


Figure 6. Distributions of the wide jet broadening, B_W , at different centre-of-mass energies together with perturbative QCD predictions combined with power corrections or traditional hadronization corrections.

power corrections prove to be surprisingly successful. The approach is rather economical in the sense that only one additional universal parameter α_0 needs to be determined by experiment. A number of examples have recently been given, where also the limitations and difficulties became apparent.

5. FRAGMENTATION IN DIS

In the above jet analyses, the emphasis is placed on accessing the very rare multi-jet events at increasingly large jet E_T to minimize soft non-perturbative effects in the subsequent comparison to perturbative QCD predictions. Valuable information on the properties of QCD can also be gained from the study of charged particle production, however, which is obviously strongly influenced by the non-perturbative hadronization phase. A key question is: To what extent do the measured hadrons reflect the underlying par-

ton spectra? These depend on the initial partonic configuration and the subsequent parton cascade. The typical observables are particle rates, momentum distributions of the hadronic final state particles and multi-particle correlation variables. Increasingly refined perturbative predictions for more and more complex observables have been derived within the framework of the Modified Leading Log Approximation (MLLA) [21]. Many of those predictions have been compared with data using the concept of Local Parton-Hadron Duality (LPHD). The hypothesis of LPHD in connection with MLLA relates the average properties of partons and hadrons by means of a simple normalization constant. With these assumptions, the theoretical predictions depend essentially on two parameters only, an effective strong coupling constant determined by the QCD scale Λ and an energy cutoff parameter Q_0 . Both have to be determined by measurement.

A recent measurement of scaled momentum

distributions [23] is presented in Fig. 7, where the mean value and higher moments of the ξ distribution are shown as a function of Q^2 for different ranges of x . The variable ξ is defined as $\ln 1/x_p = \ln Q/2p^{Breit}$. Only particles in the current hemisphere of the Breit frame are considered. This makes possible a direct comparison with results from e^+e^- annihilation, which are also included in the figure.

The fair agreement observed between the results of DIS and e^+e^- annihilation suggests that the main features of quark fragmentation are universal. While the mean value of the ξ distribution as a function of Q^2 is well described by MLLA predictions, no consistent description of mean, width, skewness and kurtosis can be achieved. The measurements benefit considerably from the large range in Q^2 that is now covered by HERA. Clearly, further studies, possibly considering mass effects [25], are needed to understand this disagreement.

Measurements of the properties of particles in the target hemisphere have also been made and the correlation between the mean particle multiplicity in the two hemispheres has been studied [23].

A measurement of the charged particle x_p distribution as a function of Q is shown in Fig. 8 for different ranges in x_p [24]. QCD calculations in NLO combined with NLO fragmentation functions are compared to the measurement. For large values of x_p and with increasing Q , a significant decrease of the distributions is observed, which is expected from scaling violations in the fragmentation functions due to gluon radiation. The agreement with the prediction is good, except at small values of x_p where mass effects, which are not considered in the calculations, are important. A simple power correction ansatz as proposed in [27] results in a surprisingly close description of the data. Detailed calculations of these power corrections have been started and were discussed at this meeting [26].

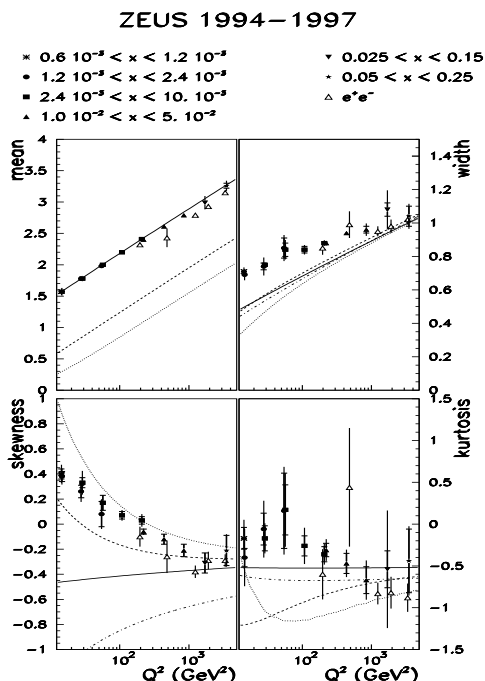


Figure 7. Evolution of the mean, and of the higher moments skewness and kurtosis, of the $\ln(1/x_p)$ distribution with Q^2 .

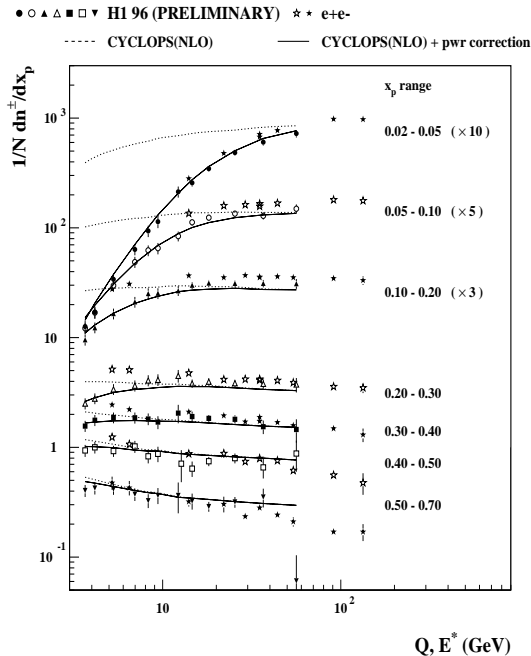


Figure 8. The inclusive charged particle distributions $1/N_{DIS}dn^{\pm}/dx_p$ in the current hemisphere of the Breit frame. The distribution is shown as a function of Q for different intervals of x_p . Data from e^+e^- annihilation as a function of the centre-of-mass energy E^* are also shown.

6. FORWARD JET AND π^0 PRODUCTION IN DIS

The study of jet and particle production in the very forward (proton) region in DIS is largely motivated by the interest in the parton dynamics at small values of x . In particular, one would like to access a region where the validity of the BFKL equations could be tested.

Experimentally, measurements close to the edge of the detectors are challenging, but both H1 and ZEUS [28] have nevertheless succeeded to measure forward jet cross sections. They show a significant rise of the forward jet cross section with decreasing values of x . The measurements are in striking disagreement with the predictions of Monte Carlo models based on the traditional

DGLAP parton showers. Furthermore, QCD predictions in NLO disagree with the data [29].

Recently, several ways to describe the measurement have been found and were presented at this meeting [30, 32, 31]. These are: the inclusion of a resolved *virtual* photon contribution in the NLO calculations performed by [30]; the inclusion of a resolved *virtual* photon component in the Monte Carlo model RAPGAP [28]; and the inclusion of NLO effects in a recent BFKL calculation by applying higher order consistency conditions [32]. In addition, [31] obtained a good description of forward jets (and of F_2) with a modified version of the Monte Carlo program SMALLX based on the CCFM parton evolution equation.

An important new measurement of forward π^0 cross sections was presented in [33]. Differential distributions in x , η_{π} and $p_{t,\pi}$ have been measured for three ranges of Q^2 . Given the difficult phase space region, the precision of the measurement is excellent and compares favourably with the jet measurements. The inclusive π_0 cross sections as a function of x are shown in Fig. 9. Again, RAPGAP with a resolved virtual photon contribution describes the data better than MC models based on DGLAP parton showers such as LEPTO (shown). The best description is obtained by the modified BFKL calculation mentioned above.

In conclusion, significant theoretical progress has been made in understanding the physics of the forward region. The precise measurement of the multi-differential π^0 distributions will constrain existing and future models considerably.

7. REAL PHOTON STRUCTURE

In a hard collision involving an incoming photon, this photon may scatter directly, or it may first fluctuate into a hadronic object. Although it is no longer considered possible to make a complete prediction of the photon's structure without input from experiment, measurements that are sensitive to the hadronic nature of the photon can nevertheless provide a test of some fundamental hypotheses.

In e^+e^- collisions, the photon's structure function F_2^{γ} is probed in deep inelastic scattering

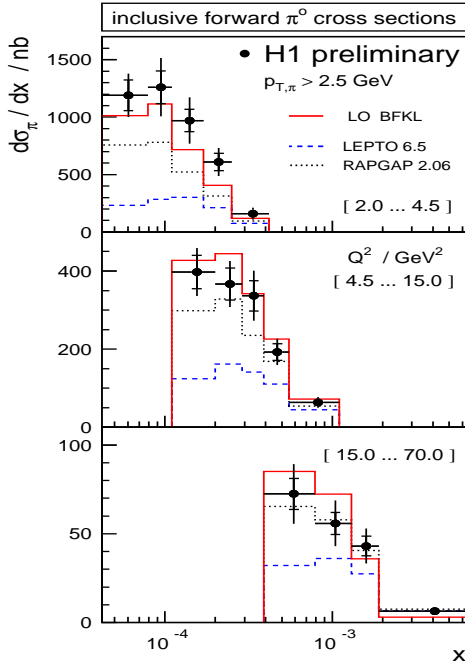


Figure 9. The inclusive π^0 cross sections as a function of x for three ranges of Q^2 , together with the predictions of MC models and the BFKL calculation of [32].

processes where one of the leptons is scattered through a large angle. F_2^γ is expressed as a function of the fraction of the photon's energy participating in the scatter, x , at the resolution scale provided by the square of the momentum transfer at the scattered lepton vertex, Q^2 . Fig. 10 shows the latest world measurements of $F_2^\gamma(x)/\alpha$ at medium Q^2 [34]. The available photon parton density parametrizations are generally able to describe the data.

At HERA, the partons of the proton probe directly, not only the quark density, but also the gluon density of the photon. Here the resolution scale of the probe is measured in terms of the transverse momenta of the jets or tracks produced. In Fig. 11 an extraction of the leading order gluon density of the photon is shown [35]. Here the probing resolution for the jet analysis is $\langle P_T^2 \rangle = 74 \text{ GeV}^2$ and for the track analysis $\langle P_T^2 \rangle = 38 \text{ GeV}^2$. The different experimental ap-

proaches both indicate a rise of the leading order gluon density as x_γ falls.

At high values of the resolution power it becomes possible to describe the high- x quark component of the photon's structure using quark parton model predictions alone, as shown in Fig. 12 [34]. The experimental constraint on the photon's structure coming from the e^+e^- experiments, however, grows weak here.

ZEUS has measured dijet cross sections in photoproduction in this high scale region ($E_{T\text{leading, second}}^{\text{jet}} > 14, 11 \text{ GeV}$) as shown in Fig. 13 [36]. Next-to-leading order perturbative QCD calculations using current photon parton densities are unable to describe these data when both jets are in the central region, $0 < \eta_{1,2}^{\text{jet}} < 1$. As other uncertainties are expected to be low in this kinematic regime, it would be a good test of our understanding of photon-induced processes to check whether a parton density can be found which allows the ZEUS data to be described while remaining consistent with the available high- Q^2 F_2^γ measurements from LEP.

An interesting alternate process, which may reveal information on the photon's structure, comes from prompt photon production in $\gamma\gamma$ and γp collisions. Prompt photon cross sections have

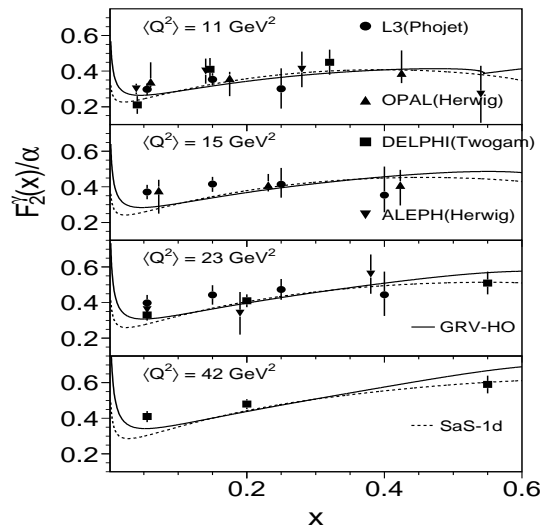


Figure 10. F_2^γ/α at medium Q^2 from LEP.

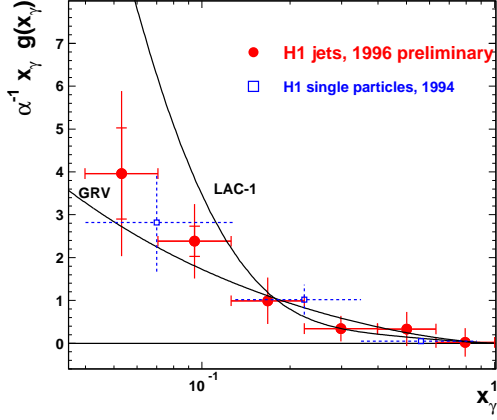


Figure 11. Measurement of the gluon density in the real photon from dijet and high p_T track events.

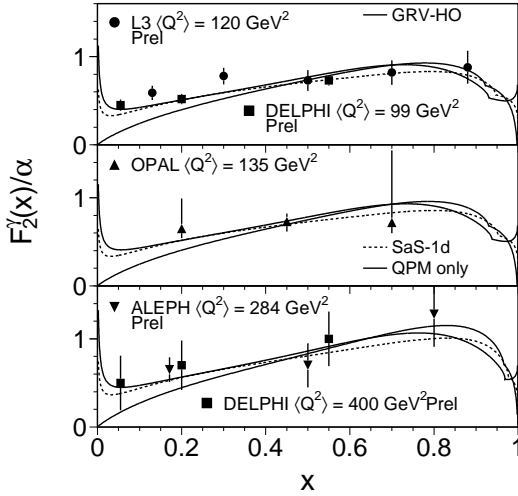


Figure 12. F_2^γ/α at high Q^2 from LEP.

the potential to be free of theoretical uncertainties arising from hadronization effects. Both the ZEUS [37] and TOPAZ [38] collaborations presented early studies of prompt photon production but a considerable improvement in statistics is necessary before any strong conclusions may be drawn.

8. VIRTUAL PHOTON STRUCTURE

It is expected that as a photon's virtuality increases, it will begin to lack the time to develop a complex hadronic structure.

From the total cross section for the double-tag process, $e^+e^- \rightarrow e^+e^-\gamma^*\gamma^* \rightarrow e^+e^-X$, there is an indication that the hadronic component of the photon's structure is still evident at sizeable photon virtualities [39].

ZEUS has measured the ratio of the low- x_γ dijet cross section to the high- x_γ dijet cross section as a function of the photon's virtuality Q^2 at the probing scale provided by $E_T^{\text{jets}} > 5.5$ GeV, Fig. 14 [36]. This ratio is flat for a parton density that does not evolve with Q^2 (GRV LO) and falling for a parton density that is suppressed with Q^2 (SaS 1D). Therefore the fall that is observed in the data indicates that the photon's parton density is suppressed as the photon's virtuality increases.

H1 present the effective parton density of the photon, \tilde{f}_γ , as a function of Q^2 in Fig. 15 [35]. The data are consistent with parton densities which fall logarithmically with Q^2 and are inconsistent with a pure vector meson dominance

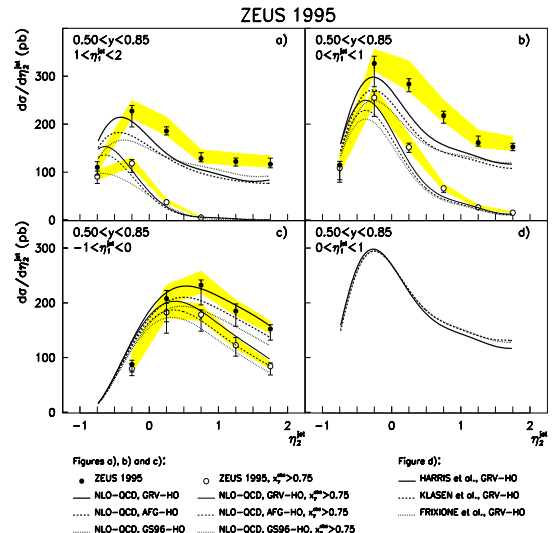


Figure 13. Dijet cross section as a function of η_2^{jet} in bins of η_1^{jet} and for $0.50 < y < 0.85$.

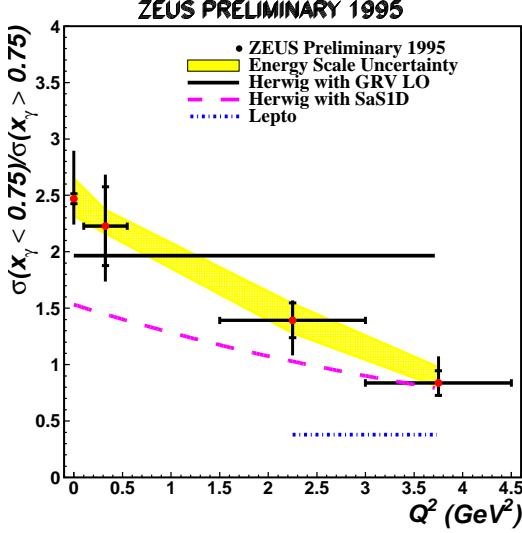


Figure 14. Ratio of the dijet cross section for $x_\gamma^{\text{OBS}} < 0.75$ to the dijet cross section for $x_\gamma^{\text{OBS}} > 0.75$.

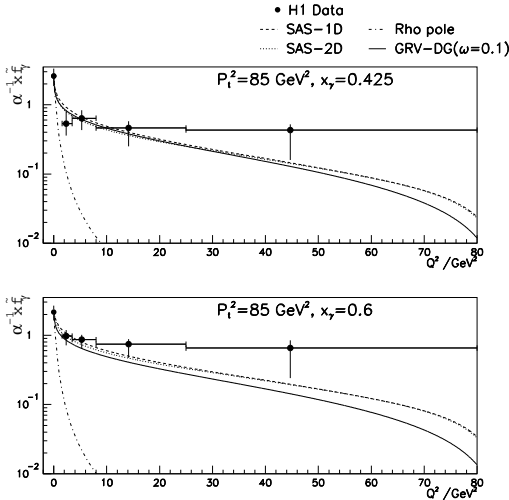


Figure 15. Leading order effective parton density of the photon as a function of Q^2 at $P_T^2 = 85 \text{ GeV}^2$.

ansatz for the photon's structure.

9. JET SUBSTRUCTURE IN PHOTON-INDUCED COLLISIONS

The measurement of jet substructure in photon-induced collisions has been used to study universal properties of fragmentation.

Jet shapes measured in deep inelastic scattering and in $\gamma\gamma$ collisions are compared in the top row of Fig. 16 [38]. The comparison is made

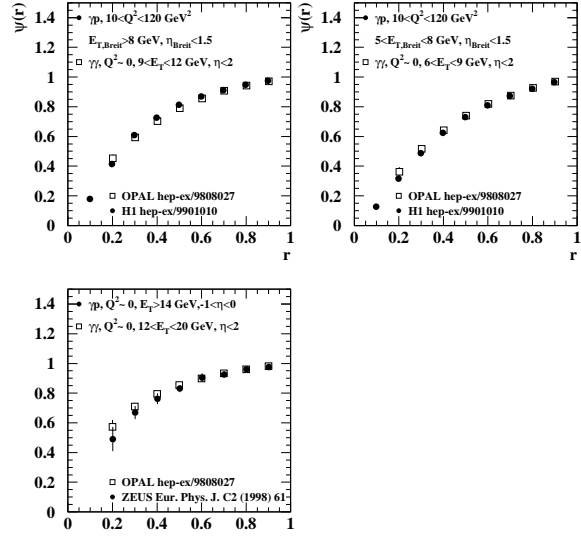


Figure 16. Jet shapes in dijet events measured by OPAL, H1 and ZEUS.

for measurements of similar E_T^{jet} and a universality of fragmentation in jets is observed. In the bottom plot of this figure a comparison is made between jets in $\gamma\gamma$ collisions and in γp collisions. The jets from the γp collisions are narrower, but this could be due to the slightly larger E_T^{jet} of the γp measurement.

Using a clustering algorithm based on the relative transverse momentum of particles, it is possible to resolve subjets within jets in a well-defined manner. The number of subjets will depend upon the value of the resolution parameter, y_{cut} , with which one looks into the jet. In Fig. 17 the mean number of subjets at resolution parameter $y_{\text{cut}} = 0.01$ is shown as a function of jet pseudo-

rapidity [37]. It is found that $\langle n_{\text{subject}} \rangle$ increases

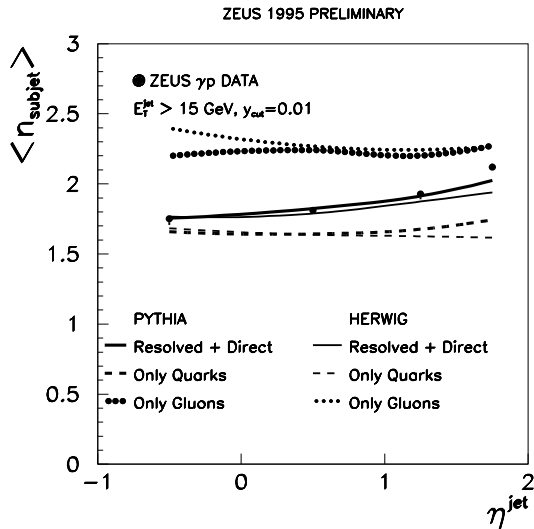


Figure 17. Number of subjects at $y_{\text{cut}} = 0.01$ as a function of η^{jet} .

as expected from the predominance of gluon jets in the forward region.

10. INCLUSIVE PHOTONS IN $p\bar{p}$ COLLISIONS

Inclusive photon results from the Tevatron were presented, where the CDF and DØ data were seen to be consistent with each other [40]. The CDF data reach lower photon p_T values where the cross section tends to be higher than theory calculations. This shape difference is difficult to explain with current NLO QCD calculations. Best fits are obtained with the k_T smearing procedure used to explain the E706 photon data. A k_T smearing of about 3.5 GeV is needed to explain the data. The result is shown in Fig. 18. In the same talk a high statistics measurement of photon-muon production was also presented, which compares well with NLO QCD.

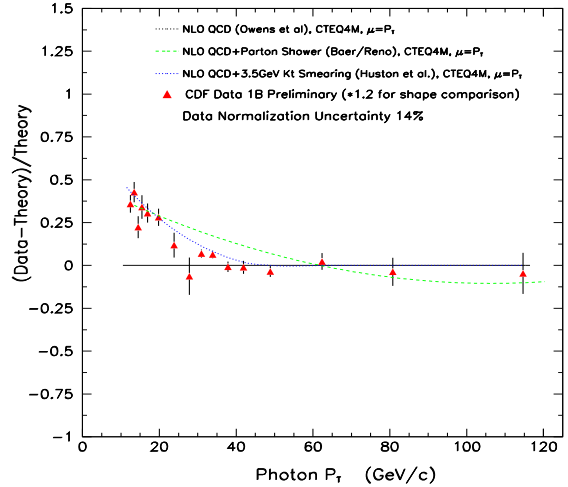


Figure 18. The CDF measurement of the inclusive photon p_T spectrum.

11. JET RESULTS FROM THE TEVATRON

Results were presented on subjet multiplicity in quark and gluon jets at DØ [41]. Jets are identified using the k_T jet algorithm, which has the advantage of being IR-safe and allows a more direct comparison between theory and measurements. The gluon jet fraction was determined at $\sqrt{s} = 1800$ GeV and $\sqrt{s} = 620$ GeV. The results indicate that there are more subjects at $\sqrt{s} = 1800$ GeV as well as more subjects in gluon jets.

In the joint session with the structure function working group, both CDF and DØ presented results on the inclusive jet cross section [42] [43]. When the CDF run IA results were published, they showed an excess of events at high E_T with respect to QCD expectations using particular parton density functions. This excess generated a lot of interest, and explanations ranged from quark substructure to modified parton density functions. The preliminary CDF measurement from the IB run is based on an integrated luminosity of 87.7 pb^{-1} and is in agreement with the Run IA measurement. DØ presented recently published results which are consistent with QCD predictions. Improved energy calibrations at DØ allowed them to reduce the systematic errors to

10% at low E_T and to about 30% at high E_T . A comparison of CDF data with DØ data is shown in Fig. 19, where the results are seen to be consistent. It appears that the behaviour at high E_T

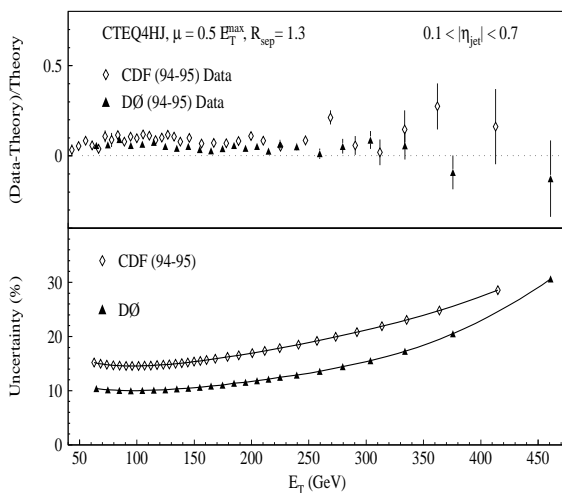


Figure 19. The CDF and DØ measurements of the inclusive jet cross section.

can be accommodated by enhancing the gluon at high x as is done in the CTEQ PDFs. A more sensitive search for quark substructure can be conducted using either the dijet mass distribution or dijet angular distribution and will be discussed later.

A consistency check of α_s from jet data was presented by CDF [43]. The technique extracts α_s from a third-order equation where the coefficients are calculated assuming a particular PDF and value of α_s . By varying α_s one can check for a consistent solution where the extracted α_s equals the input value. The method depends on the choice of PDF since different PDFs result in a different α_s . The results show the running of α_s in one experiment and yield a result consistent with measured α_s from other experiments.

Both CDF and DØ presented the ratio of the scaled cross section for a centre-of-mass energy of 630 and 1800 GeV as a function of x_T [42] [43]. The ratio allows a reduction of the uncertainty

due to theory and experiment. Above values of $x_T = 0.1$ the CDF and DØ measurements agree, while at lower x_T values the measurements diverge. The DØ data tend to higher ratio values while the CDF results tend to lower values as is shown in Fig. 20.

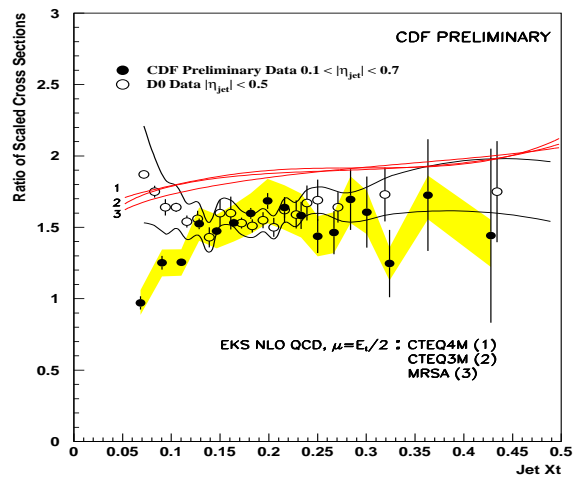


Figure 20. Ratio of the scaled cross section for centre-of-mass energies of 1800 and 630 GeV as a function of x_T as measured by CDF and DØ.

DØ also presented the rapidity dependence of the inclusive jet cross section for three different η bins up to $\eta < 1.5$ [42]. Results were in good agreement with NLO QCD calculations.

Both CDF and DØ presented measurements on the dijet mass distribution [44] [45]. Results from the two experiments are in good agreement in both shape and normalization. DØ has used the measurement to place limits on quark compositeness as is shown in Fig 21. Dijet angular distributions provide a sensitive test of new physics and have the advantage that the distributions are less sensitive to the energy measurement uncertainty. Results were presented from CDF and used to place limits on quark compositeness.

DØ presents the differential dijet cross section separately for opposite-side jets and same-side

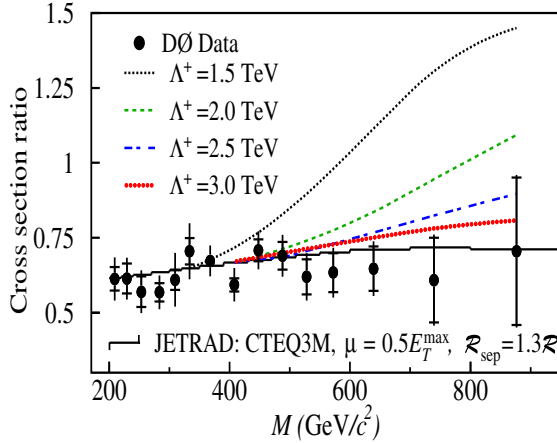


Figure 21. Limits placed on compositeness models using the DØ dijet mass data

jets [44]. Both jets are required to sit in the same η bin. Results were compared to the JETRAD calculation using different PDFs. Dijet differential cross sections from CDF were shown where the central jet was used to measure the E_T of the event [45]. A second jet is allowed to fall in one of four η bins. A quantitative comparison of different PDFs is under way. The differential dijet measurement covers a plane in the x - Q^2 space, making it more sensitive to the shape of the cross section determined by different PDFs. The data will provide a useful input to QCD fits in order to determine refined PDFs.

12. CONCLUSIONS

At this meeting many beautiful, high-precision experimental results were presented and compared with theoretical predictions. QCD has been clearly established as a successful theory for the description of hard scattering processes. It is now increasingly important to better understand soft non-perturbative phenomena and processes where more than one hard scale plays a part. The further development of power corrections and resummed calculations as well as the calculation of QCD cross sections at next-to-next-to-leading order is under way. This program will eventu-

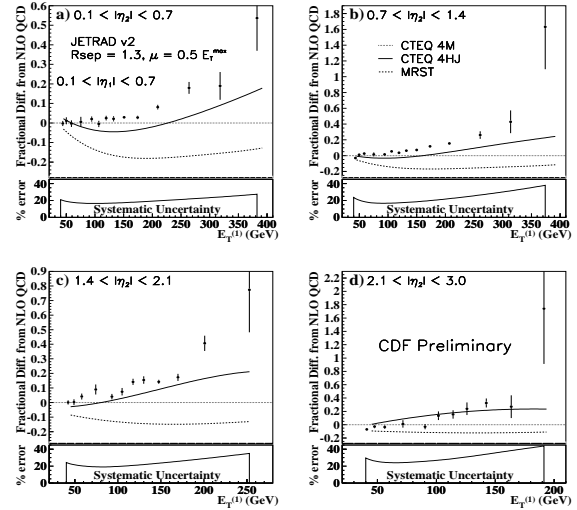


Figure 22. Triple differential dijet cross section.

ally lead to an even more stringent comparison of theory and experiment. The development of these concepts should benefit greatly from continued close communication between theorists and experimentalists.

REFERENCES

1. R. Gerhards, these proceedings.
2. Y. Eisenberg, these proceedings, hep-ex/9905008.
3. S. Frixione, these proceedings, hep-ph/9905545.
4. M. Wing, these proceedings, hep-ex/9905051.
5. P. Newman, these proceedings.
6. S. Mohrdieck, these proceedings.
7. H1 Collaboration, T. Ahmed *et al.*, Phys. Lett. **B346** (1995) 415.
8. ZEUS Collaboration, M. Derrick *et al.*, Phys. Lett. **B363** (1995) 201.
9. H1 Collaboration, C. Adloff *et al.*, Eur. Phys. J. **C5** (1998) 4, 625.
10. H1 Collaboration, C. Adloff *et al.*, Eur. Phys. J. **C6** (1999) 4, 575.
11. N. Tobien, these proceedings.
12. Proceedings of the HERA Monte Carlo Workshop 98/99, to be published.

13. M. Wobisch, these proceedings.
14. H1 Collaboration, C. Adloff *et al.*, *Measurement of Dijet Cross Sections in Deep-Inelastic Scattering at HERA and a Direct Determination of the Gluon Density in the Proton*, contributed paper to ICHEP98, Vancouver, Canada, July 1998.
15. E. Tassi, these proceedings.
16. K. Rabbertz, these proceedings, hep-ex/9906002.
17. Yu.L. Dokshitzer, A. Lucenti, G. Marchesini and G. P. Salam, Nucl. Phys. **B511** (1998) 396 and JHEP **05** (1998) 003.
18. Yu. L. Dokshitzer, G. Marchesini, G. P. Salam, hep-ph/9812487.
19. H1 Collaboration, C. Adloff *et al.*, Phys. Lett. **B406** (1997) 256.
20. G. Dissertori, these proceedings, hep-ex/9904033.
21. see e.g. V.A. Khoze and W. Ochs, Int. J. Mod. Phys. **A12** (1997) 2949.
22. Ya.I. Azimov, Yu.L. Dokshitzer, V.A. Khoze and S.I. Troyan, Z. Phys. **C27** (1985) 65.
23. L. Zawiejski, these proceedings, hep-ex/9905061.
24. D. Kant, these proceedings.
25. S. Lupia and W. Ochs, Eur. Phys. J. **C2** (1998) 307.
26. M. Dasgupta and G.E. Smye, these proceedings.
27. Yu.L. Dokshitzer and B.R. Webber, discussion at the 3rd UK Phenomenology Workshop on HERA Physics, Durham, UK, 1998.
28. ZEUS Collaboration, J. Breitweg *et al.*, Eur. Phys. J. **C6** (1999) 4, 239; H1 Collaboration, C. Adloff *et al.*, Nucl. Phys. **B538** (1999) 3.
29. E. Mirkes and D. Zeppenfeld, Phys. Rev. Lett. **78** (1997) 428.
30. G. Kramer and B. Poetter, hep-ph/9901314.
31. H. Jung, these proceedings.
32. J. Kwiecinsky, A.D. Martin and J.J. Outhwaite, hep-ph/9903439.
33. T. Wengler, WG3-23, hep-ex/9905062.
34. K. Freudenreich, these proceedings.
35. J. Cvach, these proceedings, hep-ex/9906012.
36. N. Macdonald, these proceedings.
37. K. Umemori, these proceedings.
38. S. Söldner-Rembold, these proceedings, hep-ex/9906014.
39. V. Andreev, these proceedings.
40. S. Kuhlmann, these proceedings.
41. R. Snihur, these proceedings.
42. D. Elvira, these proceedings.
43. A. Akopian, these proceedings.
44. H. Schellman, these proceedings, FERMILAB-Conf-99/170-E.
45. F. Chlebana, these proceedings, FERMILAB-Conf-99/172-E.